

Clathrate Formation in Water–Cyclic Ether Systems at High Pressures*

YU. A. DYADIN**, F. V. ZHURKO, I. V. BONDARYUK, and G. O. ZHURKO

Institute of Inorganic Chemistry of the USSR Academy of Sciences, Siberian Branch, Novosibirsk 630090, U.S.S.R.

(Received: 4 December 1989; in final form: 12 January 1990)

Abstract. Experimental data on the investigation of the water–trimethyleneoxide system, P, t, x phase diagram (up to 6 kbar) are presented. The results are compared with those on water systems with ethyleneoxide, 1,3- and 1,4-dioxane, 1,3-dioxolane and tetrahydrofuran, on the basis of which a summarized P, t, x diagram is plotted for water–cyclic ether systems. It is shown that in all the systems in which a cubic structure II hydrate forms at 1 bar, it eventually turns to cubic structure I under pressure. The nature of high pressure hydrates is discussed.

Key words. Clathrate hydrates, high pressure clathrate formation, cyclic ether, P, t, x phase diagram

1. Introduction

Cyclic ethers are remarkable because, by systematically changing the dimensions of these molecules, one can follow the course of clathrate formation in the series of polyhydrates as it transforms from cubic structure II (CS-II) to cubic structure I (CS-I) via the water–trimethyleneoxide (TMO) system, where compounds of both structures are formed [1–4].

The ethyleneoxide (EO) cyclic ether hydrate was first discovered in 1922 [5]. Palmer seems to have been the first to observe the hydrate of tetrahydrofuran (THF) in 1949 [6]. Later the phase diagram with THF was studied by the authors of [7] and [8]. The structures of ethyleneoxide polyhydrate and the double hydrate of THF have been determined [9, 10]. Gough and Davidson [11] were the first to apply high pressures (up to 6 kbar) to the investigation of cyclic ether clathrate hydrates and to show that the $\text{THF} \cdot 17 \text{H}_2\text{O}$ hydrate was destabilized by pressure.¹

Table I, citing the data on the composition, thermal stability and unit cell parameters of several clathrate hydrates of cyclic ethers shows that their ability to form CS-I or CS-II clathrate compounds depends upon the guest molecule dimensions. The thermal stability of the hydrates depends on the correspondence between the dimension of the guest and of the CS-I or CS-II cavities.

The unlimited solubility of liquid cyclic ethers in water, which simplifies² the study of equilibria at high pressures excluding the interphase mass transfer, the slowest clathrate formation stage, is advantageous for our investigation of clathrate formation under pressure. Binary water systems with tetrahydrofuran [13], 1,3-

*Dedicated to the memory of D. W. Davidson.

**Author for correspondence.

Table I. Some characteristics of clathrate hydrates of cyclic ethers based on the data of different authors.

Hydrate	Guest molecule dimensions [^a]	Hydrate structure	Unit Cell parameters ^b Å	Congruent (c) incongruent (i) melting point, °C	References
EO · 6.9 H ₂ O	5.5	CS-I	12.03 (-25°C)	11.1;c	3, 5, 31, 32
TMO · 7.7 H ₂ O	6.1	CS-I	12.13* (-50 + -60°C)	-20.6;i	2, 3, 4, 21, 49, 52
TMO · 17 H ₂ O		CS-II	17.22	-9.2;i	1, 3, 21, 33
1,3-DO · 17 H ₂ O	6.2	CS-II	17.25	-2.6;c	1, 3, 14, 26, 51
THF · 17 H ₂ O	6.3	CS-II	17.28 ^d	4.3;c	1, 6, 7, 8, 13, 33, 50
1,3-DX · 17 H ₂ O ^e	7.1	CS-II	17.36	-3.5;c	3, 15, 34, 35, 51
1,4-DX · 17 H ₂ O ^e	7.2	CS-II	17.41	-11.3;i	3, 36, 37.

*In reference [4] the values of 12.2 (-130°) and 12.15 (-30°) are presented.

^a [is the maximum size, calculated on the basis of the initial data: molecule geometry [38] and van der Waals radius [39]. The dimensions cited here differ from those given in [1]. We present the maximum length. For instance, in 1,4-dioxane the distance from one equatorial hydrogen to the other across the inversion center is 7.2 Å, while the projection of this line on the plane across four carbon atoms is 6.7 Å. This was noticed by the authors of [55] who give the maximum TMO molecule value 6.2 Å, while the value of 5.5 Å given previously is the projection of this line on the plane, crossing the centres of the atoms CCCC (according to our calculations 6.1 and 5.6 Å, respectively). For 1,3-dioxolane and tetrahydrofuran in the given range projection of the maximum molecule length line on the plane of the 4 atoms (the fifth one is not on the plane [38]) agrees with the lengths of [1]. Of all the CS-II hydrates the highest melting point of the THF · 17 H₂O hydrate is best explained by the dimensions presented by us while, on the basis of the results presented previously one should expect the highest melting point for dioxane hydrates, whose dimensions would correspond to the H-cavity free diameter (6.6 Å) [24].

^b For CS-II, parameters are standardized to 0°C [26], and for CS-I the temperature at which parameters were obtained is given in brackets.

^c In reference [3] for hydrate 1,3-DO a melting point of -50°C is given.

^d The thermal expansion in the range of 18-250 K was determined by Tse *et al.* (cited from [26]).

^e D. Davidson's detailed analysis of CS-II hydrate compositions [11, 24] shows these hydrates to have compositions which practically do not differ from the ideal one, i.e. 1 : 17. So the results obtained for the compositions of dioxane 1 : 34 [3], 1 : (36-39) [36] and 1 : 25 [34] hydrates arouse interest because they were quite unexpected. However, these results have not been confirmed: the authors of [37, 54] have shown dioxanes to form CS-II hydrates without any anomalies. Prof. D. Davidson had kindly informed us about these results before work [37] was published. Later we have corroborated these conclusions and shown in [3, 36] the large hydrate numbers of 1,4-dioxane hydrate to be associated with treatment of thermograms for nonequilibrium state. In [34] the uncertainty of the results was probably caused by atmospheric gases [15].

dioxolane [14], 1,3- and 1,4-dioxane (1,3- and 1,3-DX) [15, 16] and the melting curve of ethyleneoxide (EO) polyhydrate under pressure [17] have been studied earlier. The present work discusses the water-trimethyleneoxide system at high pressures. An attempt is also made to summarize the data on clathrate formation under pressure in a series of water systems with guest molecules ranging from ethyleneoxide to 1,4-dioxane.

2. Experimental

2.1. REAGENTS AND TECHNIQUES

Trimethyleneoxide was synthesized from 1,3-propanediol by a two-step method described in [18]. During the first stage 1,3-propanediol was treated with acetyl chloride in the presence of anhydrous calcium chloride. The 1-chloro-3-acetoxypropane obtained was separated from the excess acetyl chloride, washed with a 20% solution of sodium chloride and dried with anhydrous sodium sulphate.

Cyclization of 1-chloro-3-acetoxypropane to trimethyleneoxide (TMO) was carried out in the presence of potassium hydroxide with simultaneous distillation of the raw product. The crude TMO was dried over potassium hydroxide and purified by distillation. The fraction boiling at 47°C was collected. The content of the main product found by chromatographic analysis is not less than 98% (Chromatograph 504, Poland), $n^{20} = 1.3936$.

2.2. HIGH PRESSURE MEASUREMENTS

The apparatus is shown in Figure 1. A mixture of petroleum ether with industrial oil was used as the pressure transmitting liquid. The pressure was measured by a manganine manometer placed in the vessel at normal temperature (1) communicating with a high pressure cell (2). The manometer was made of manganine wire following the technique described in [19] and was calibrated using the known variation in the melting point of mercury under pressure [20]. The reproducibility of the pressure measurements was accurate to 10 bar. The mixture under investigation was placed into a thin-walled Teflon ampoule with a capacity of 0.1 mL (3) into which a chromel-alumel thermocouple (4) was introduced (its response is virtually independent of pressure in the range studied). The ampoule content was isolated from the pressure transmitting liquid with the help of a screw clamp (5). The reproducibility of the temperature measurements was of the order of 0.15°. The high pressure cell was cooled externally with a liquid nitrogen jacket (6), placed outside the high pressure region. A heating cell (7) with the ampoules containing the mixture under investigation (8), and a standard (9) was located inside the high pressure cell. Linear heating, cooling and maintaining constant temperature were accomplished with the aid of a precision thermoregulator RIF-101 (10). The signal from the thermocouples was delivered to the amplifier (11) and registered by the self-recording potentiometer (12). The signal from the manganine manometer (1) was delivered to the potentiometer (12) over the bridge (13). The source of the pressure was the hydrocompressor (14). The phase dia-

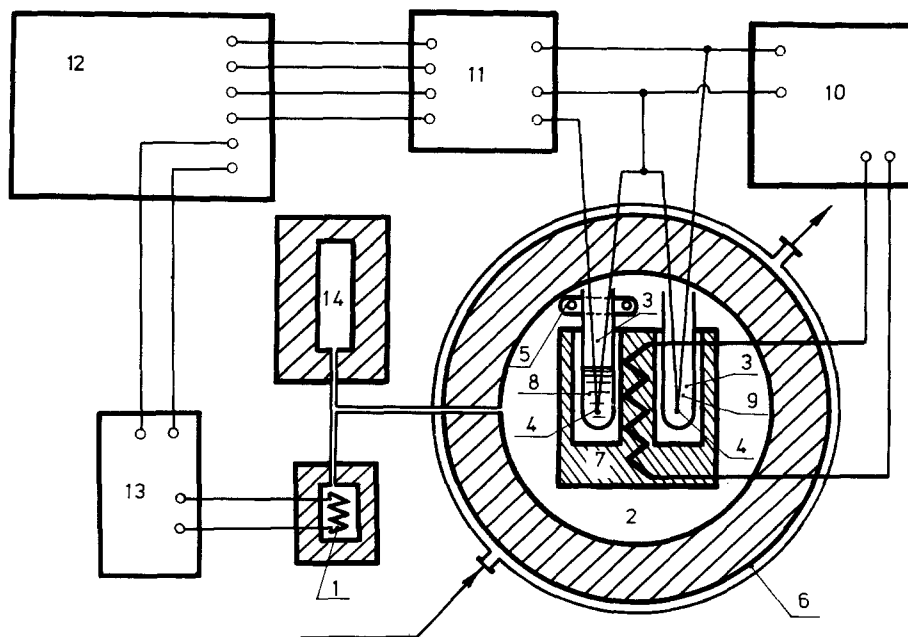


Fig. 1. High pressure installation block diagram.

gram was plotted according to the heating curves since the mixtures investigated are disposed to significant supercooling.

3. Results

3.1. WATER-TRIMETHYLENEOXIDE SYSTEM

3.3.1. Phase Diagram at Normal Pressure

A fragment of the phase diagram in the clathrate hydrates crystallization range is shown in Figure 2 (isobar 1 bar). $\text{TMO} \cdot 17 \text{H}_2\text{O}$ hydrate (h_{17}) melts incongruently according to the reaction $h_{17} \rightleftharpoons i_1 + l$ (i = ice, l = liquid phase) at -9.2°C , which agrees well with the data of [21]. The $\text{TMO} \cdot 7.2 \text{H}_2\text{O}$ hydrate (h_7) incongruent melting point at -20.6°C ($h_7 \rightleftharpoons h_{17} + l$) is also in good agreement with the data of work [21]. According to our results, the composition of the peritectic points (~ 20 and 46% by weight TMO) differ from those cited in [21] (28 and 54% TMO, respectively).

3.1.2. The Phase Diagram at High Pressure

This diagram has been plotted for 14 samples of various compositions. The heating curves of one sample were recorded at 15–20 different pressures in the range of 1 bar–6 kbar. As pressure increases, ice and CS-II hydrate are destabilized, their melting point decreases, but at different rates ($\chi \equiv (dT/dP)_{\text{melt}}$. at 1 bar for ice and

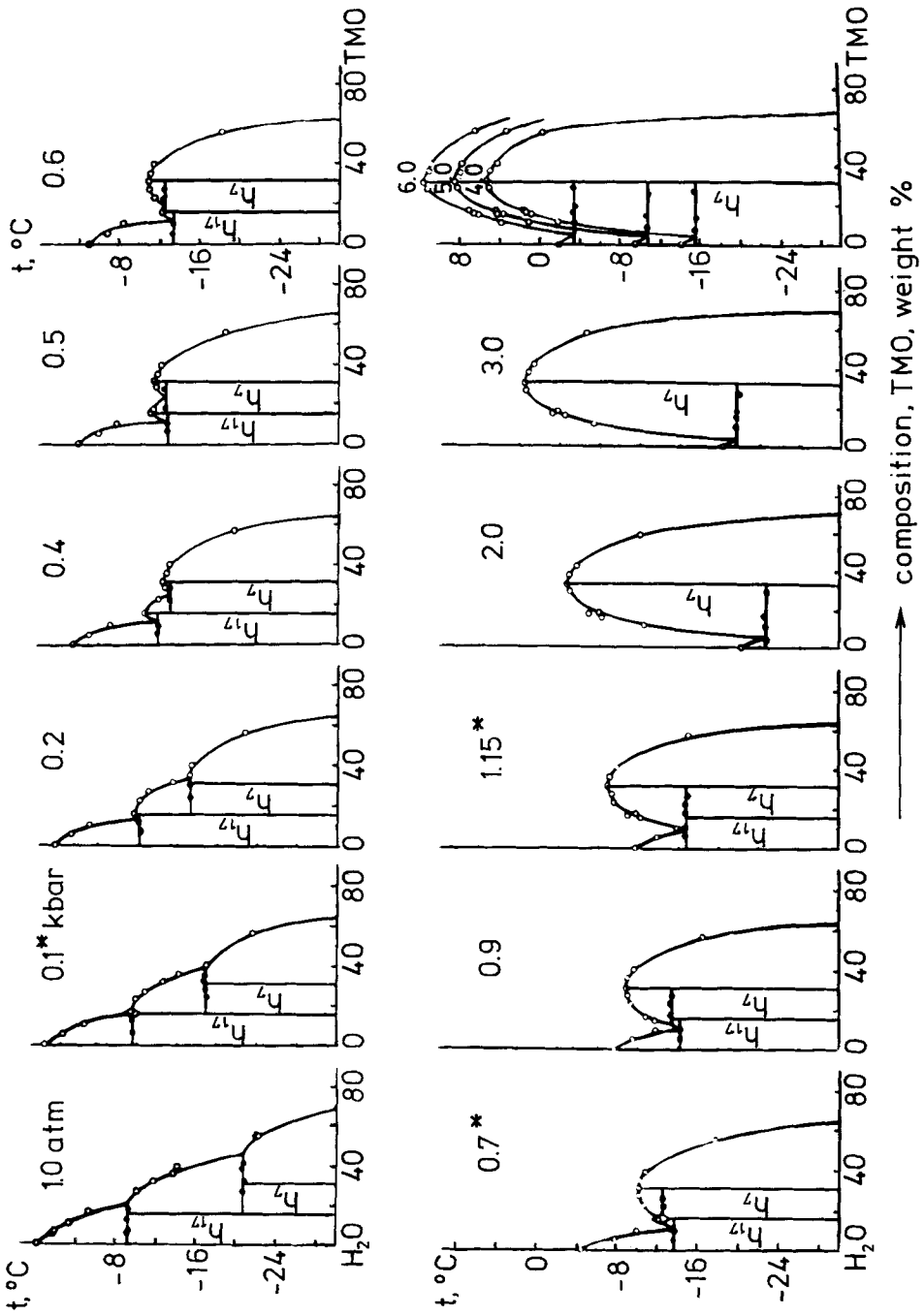


Fig. 2. Isobaric sections in the water-trimethyleneoxide system. Asterisks mark sections crossing the nonvariant point.

TMO hydrate are equal to -7.7 and $\sim -3^\circ/\text{kbar}$, respectively), which results in a more rapid ice crystallization field narrowing and the enrichment of the peritectic point with water. At $P = 0.1$ kbar its composition (15.94% TMO by weight) becomes equal to that of the hydrate. This nonvariant state is illustrated in Figures 2 and 3 (point C_{17}). At higher pressures hydrate h_{17} begins to melt congruently up to $P = 0.7$ kbar (point C'_{17}). Further pressure increase causes hydrate h_{17} to become incongruent again; however, it will melt according to the reaction $h_{17} \rightleftharpoons l + h_7$ up to 1.15 kbar (Q_4^h). At pressures above 1.15 kbar it has no crystallization field. With pressure increase the temperature of a three phase equilibrium $h_{17}h_7l$ (hydrate h_7 incongruent melting) increases sharply which results in enriching the peritectic point with water and at $P = 0.25$ kbar (point C_7) the composition of the peritectic liquid and hydrate h_7 (30.8% by TMO weight)

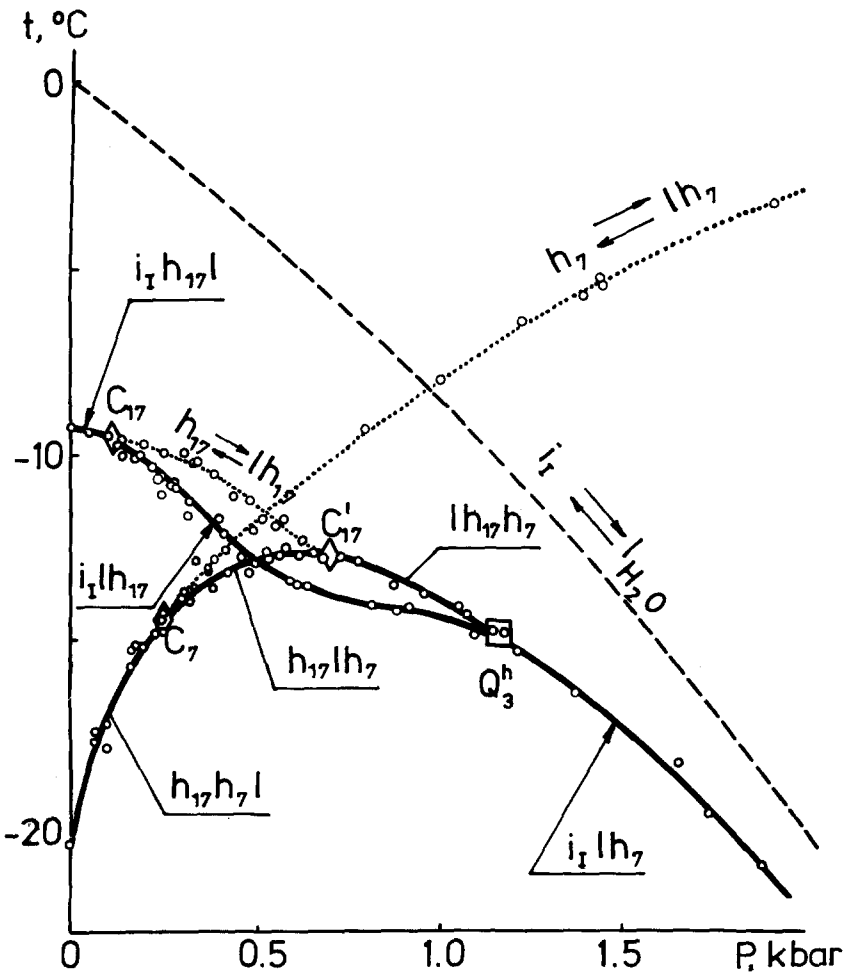


Fig. 3. P, t projection of the water-trimethyleneoxide system in the pressure range up to 2 kbar. Dashed line corresponds to the ice liquidus line, dotted line shows hydrates congruent melting. \diamond , \square are transitional and four-phase points, respectively.

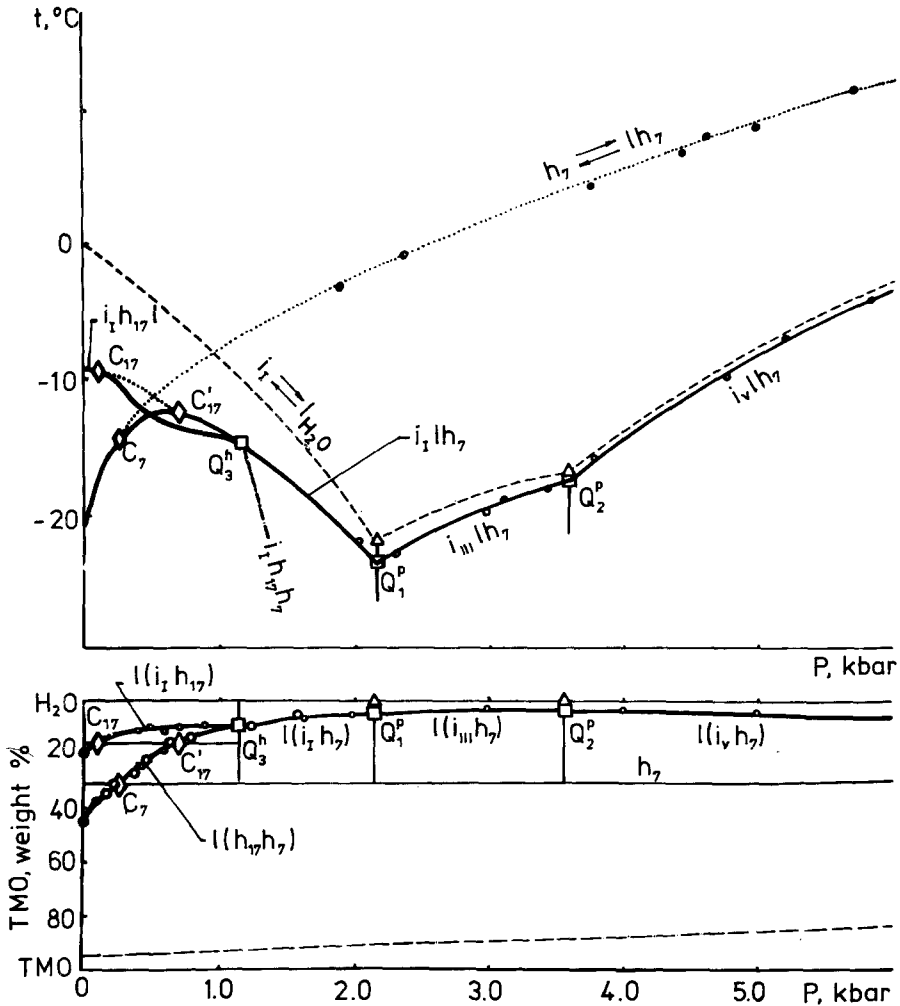


Fig. 4. P, t and P, x projections of the water trimethyleneoxide system. Δ - three phase points, - - - - assumed eutectic line abundant in trimethyleneoxide. For the rest of the designations see Fig. 3.

coincide (strictly speaking, the hydrate number is equal to 7.2). At higher pressures hydrate h_7 melts congruently, while at 6 kbar its melting point is equal to $+12^\circ\text{C}$. P, t - and P, x -projections of the phase diagram up to 6 kbar (at higher pressures the system has not been studied) are shown in Figure 4.

3.1.3. The Compositions of the Hydrates

The compositions of the hydrates were determined in the congruent melting range on the basis of the maximum on the liquidus curves in an isobaric section.

The congruent melting range of CS-II hydrate being narrow, we cannot expect our values to be of high precision. But undoubtedly, the isobars have maximum values when the composition is close to 1:17.

CS-I hydrate has its maximum when the composition is equal $1:7.24 \pm 0.43$ (the error for 95% confidence level). One might expect the maximum to shift in the direction of greater TMO content at high pressures at the expense of greater filling of the small cavities. However, with this precision level in determining the composition we have not succeeded in detecting this phenomenon.

4. Discussion

The CS-I and CS-II hydrates, having different structures behave in a different way with respect to pressure. CS-II hydrates having 8 filled³ large (H) cavities for every 16 vacant⁴ dodecahedral (D) cavities have a low packing coefficient ($k_p \approx 0.47-0.49$)⁵ [22].

Therefore, they are more or less destabilized by pressure. CS-I hydrates are much denser: even if the small cavities are empty, their relative abundance is small (2D:6T) and their packing coefficients are larger (0.52–0.54). One more property of water systems which is of importance for their study under pressure is the ability of ice to become destabilized under pressure, its degree of destabilization is greater than that of CS-II hydrates: for melting ice, as has already been mentioned, at 1 bar $\chi = -7.7^\circ/\text{kbar}$, and for CS-II hydrates it is of the order of ~ 2 to 3. Therefore, CS-II hydrate crystallization fields are most distinct under pressure, and in some cases hydrates melting incongruently at 1 bar, melt congruently under pressure, as is the case with the systems with 1,4-dioxan and TMO.

This is particularly true of CS-I hydrates stabilized by pressure. Figure 4 shows that in the system concerned the peritectic melting curve goes sharply upward under pressure up to point C_7 , where it becomes congruent, and at $P = 1$ kbar it melts at higher temperatures than ice. In all the previously studied binary systems where at normal pressure only CS-II hydrates form, at pressures equal to and above 1 kbar hydrates appear with the composition $M \cdot 7 \text{H}_2\text{O}$. In the very first work [13] ($\text{H}_2\text{O}-\text{THF}$ system) studying hydrate stoichiometry, its behaviour under pressure and modelling according to the location of the guest molecule in the cavity, it was suggested that a hydrate with this kind of stoichiometry has CS-I. Measurements of the thermophysical properties of $\text{THF} \cdot 7 \text{H}_2\text{O}$ hydrate [28–29] have shown it to be of the same clathrate nature as the 1:17 hydrate, while the 1:5 hydrate, forming at higher pressures, is not of a clathrate nature.

Figure 5 shows melting curves of 1:7 hydrates in the congruent melting pressure range. Their behaviour is seen to be similar. In our opinion this is one more convincing argument in favour of the THF, and 1,3-dioxolane (1,3-DO) hydrates having this stoichiometry as well as the ethyleneoxide and trimethyleneoxide hydrates, having CS-I.

5. Summarized P, T, X Phase Diagram of Binary Water Systems with Clathrate Formation at Normal Pressure

5.1. INCONGRUENT MELTING

CS-II hydrates capable of melting congruently at normal pressure (distectic type of diagram) or with decomposition into two liquids (syntectic type), melt at lower

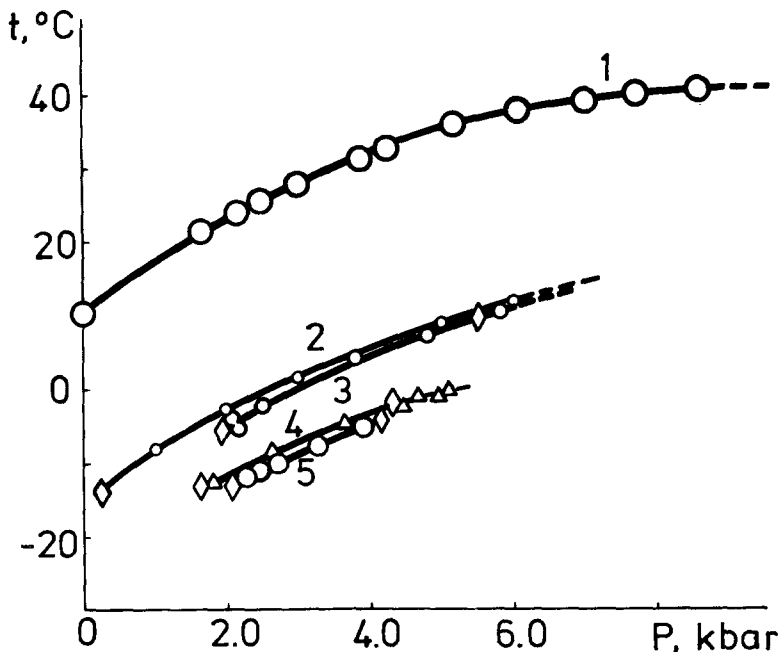


Fig. 5. Congruent melting lines of the hydrates of compositions 1 : 7; 1-EO; 2-TMO; 3-THF; 4-1,3-DO; 5-1,3-DX.

temperatures when pressure is exerted ($\chi < 0$). However, if a hydrate melts incongruently, decomposing into ice and a liquid phase more abundant in hydrate former than the hydrate itself (peritectic type), then due to ice Ih being a more porous phase than CS-II hydrate, the volume of the decomposition products can turn out to be larger than that of the hydrate. Therefore, in this case the equilibrium $h_{17} \rightleftharpoons i + l$ will shift to higher temperature with pressure increase, in which case the ice crystallization field will diminish rapidly, the peritectic solution will be enriched with water and its composition will approach that of the hydrate (the peritectic point becomes a transient one C_{17} [30]). The solution will then become more abundant in water than the hydrate (eutectic line) (Figures 6, 7).

Since, for the above reasons, clathrate formation is more distinct at high pressures, it was reasonable to start plotting a summary phase diagram with the peritectic type of isobar.

5.2. CONGRUENT MELTING

Hydrate h_{17} melting incongruently at 1 bar begins to melt congruently⁶ at point C_{17} and continues to do so under pressure until the point C'_{17} (see sections P_1 - P_4 , Figures 6, 7). At higher pressures hydrates of this structure melt incongruently (up to point Q_4^h) decomposing into CS-I hydrate (h_7) and liquid more abundant in water compared to h_{17} (section P_5). At point Q_3^h ⁷ the equilibrium $h_7 \rightleftharpoons h_{17} + l$ appears which, due to both products being less dense than hydrate h_7 , rapidly goes

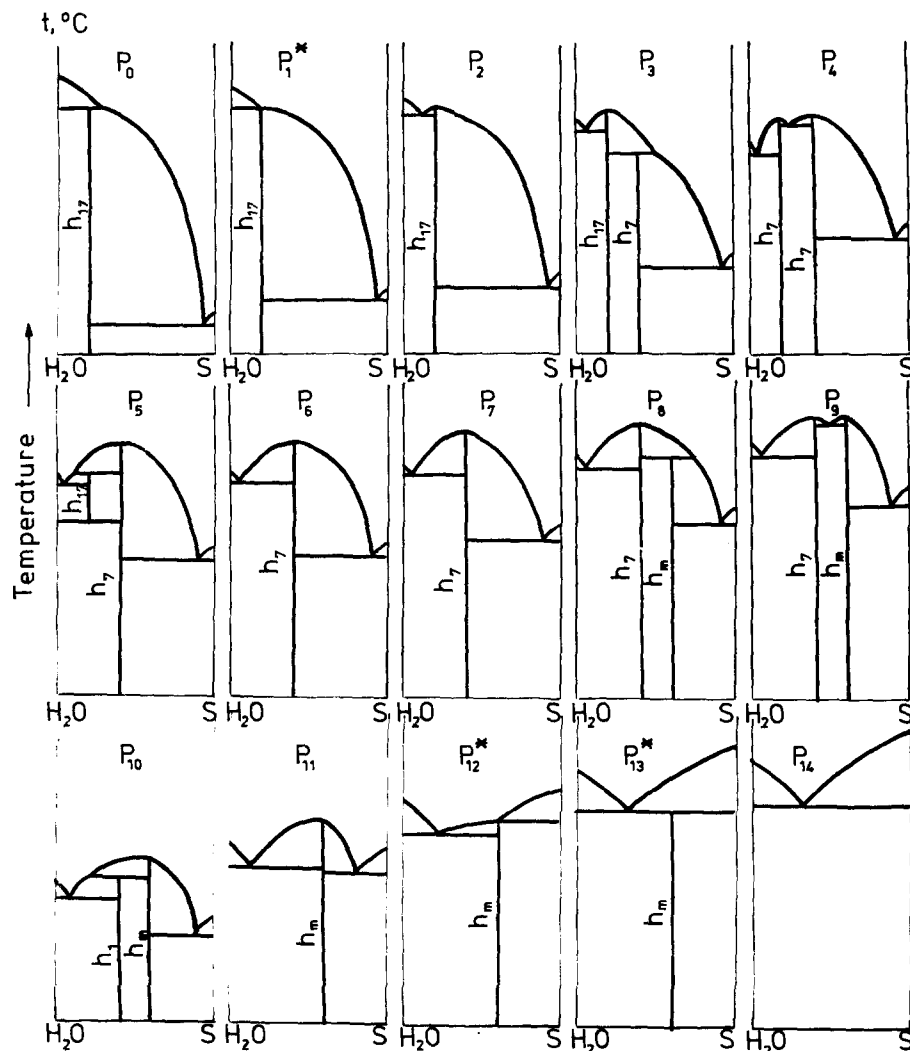


Fig. 7. Isobaric sections of the diagram depicted in Fig. 6. Asterisk marks the section crossing nonvariant points.

5.3. EUTECTIC EQUILIBRIUM

Due to the above reasons the eutectic equilibrium line with participation of ice I_h as a rule shifts downwards along the temperature axis, and to water along the composition axis, approaching the axis of a single-component 'water' system and imitating, at lower temperatures, ice melting curves. Since high pressure ices (V-VI) are already better stabilized than hydrates, the difference between the melting points of ices and eutectic mixtures increases and the eutectic composition becomes enriched with a guest. With pressure increase eutectic reactions of the hydrate former (in the case investigated) cause the eutectic equilibrium line to approach the

composition of water, moving further from the hydrate melting curves, since χ of the hydrate former is usually several times as high as that of the hydrate.

The fact that high pressure ices and crystalline guest are stabilized better than hydrates⁸, should ultimately cause the eutectic lines of both water and guest to merge, i.e. the hydrate will have no crystallization field. In the system 1,4-dioxane-water this situation is realized at $P = 4.1$ kbar, in that with 1,3-dioxane, probably, at 10.5 kbar. Upper pressure limit of the hydrates stability may be assumed to be 15–20 kbar.

In the systems concerned the hydrate crystallization field appears at the points Q_3^h (h_7) and Q_5^h (h_m). With pressure increase the equilibrium line rises along the temperature axis, and the peritectic solution composition shifts to water. The state of equilibrium $h_{17}lh_7$, establishes between points C_7 and C'_{17} , i.e. the peritectic solution changes to the eutectic one, then to the equilibrium $lh_{17}h_7$, whose temperature decreases with pressure and the peritectic equilibrium establishes again. This time, however, it is hydrate h_{17} that begins to melt incongruently. Its crystallization field comes to an end at the point Q_4^h . A similar picture is observed in the pressure and temperature range between points Q_5^h and Q_6^h . The evolution of this summarized diagram is clearly seen on the isobaric and isothermal section in Figures 7 and 8. Attention should be paid to the specific feature of isothermal sections associated with the fact that one of the hydrates (CS-II) is destabilized and the other (CS-I or h_7) is stabilized by pressure. Therefore, there is a temperature range, in which hydrate crystallization fields are separated by a homogeneous liquid phase. The main nonvariant points are presented in Table II.

6. The Effect of Guest Molecule Dimensions and Pressure on the Type of Phase Diagram Sections

As we have already mentioned, when guest molecule dimensions increase in water-cyclic ether systems, a transfer is possible from the formation of CS-I hydrates (with ethyleneoxide) to the formation of CS-II hydrates (with THF, 1,3-dioxolane, dioxane) via an intermediate system with trimethyleneoxide, in which both hydrates are formed. When the guest molecule dimensions fit the cavities of the corresponding structures well, the hydrates melt congruently and the melting temperatures are high. If, on the other hand, the molecular size slightly exceeds that of the cavity (TMO for the T-cavity, dioxans for the H-cavity), less stable hydrates and even those melting incongruently form.

Pressure is seen to have an effect similar to that of the decrease of the guest molecule dimensions. This is why we will begin by comparison with the water-1,4-dioxan system which gives the P_0 type of diagram in Figure 7. As pressure increases we pass onto the type of diagram depicted in P_2 (this type of diagram is characteristic of the system with 1,3-dioxane, tetrahydrofuran and 1,3-dioxolane⁹), then to that of P_3 , characteristic of the system in which two hydrates are crystallized, as is the case in the water-trimethyleneoxide system. And, eventually, at P_6 the type of diagram is realized which is characteristic of the water-ethyleneoxide system at 1 bar.

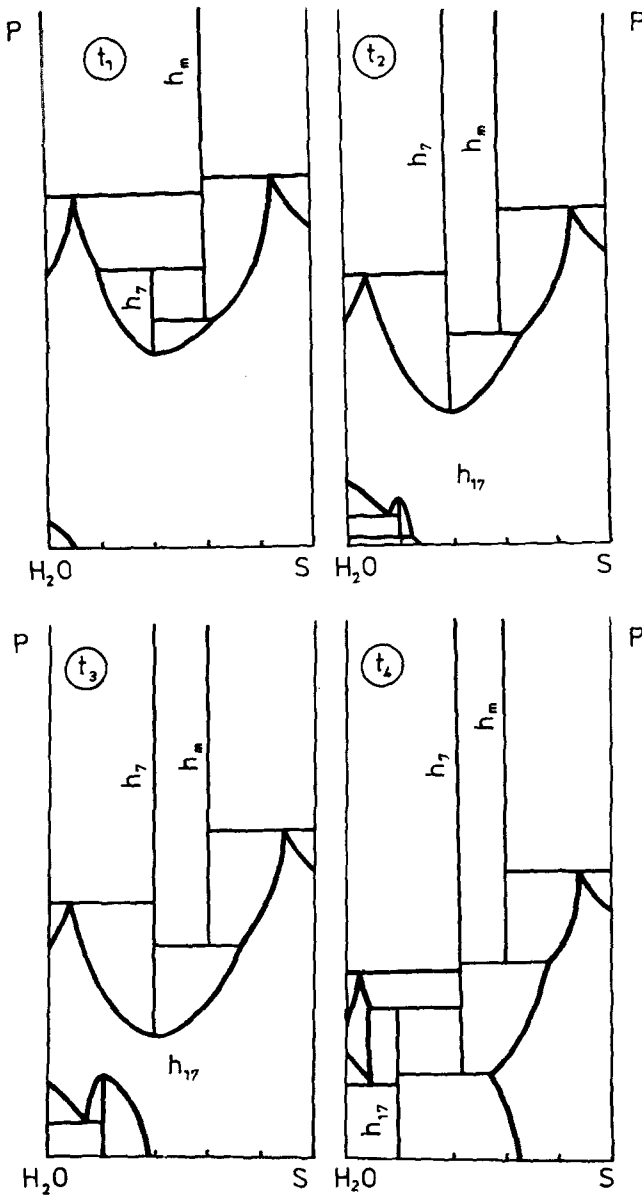


Fig. 8. Isothermal sections of the system presented in Fig. 6.

Thus the 1,4-dioxane water system¹⁰ at different pressures gives all the kinds of diagrams obtained for different guests at 1 bar.

It would be logical to expect that condensation of hydrates will proceed via hydrates of orthorhombic, hexagonal and tetragonal structures [23] which have an intermediate density (provided only big cavities are occupied) according to the

Table II. Nonvariant equilibria in the systems with cyclic ethers, where CS-II hydrates are formed at normal pressure.

Designations	Coexisting phases ^a	hydrate former				
		TMO	1,3-DO	THF	1,3-DX	1,4-DX
1	2	3	4	5	6	7
Q ₃ ^h	$h_{17}h_7ls^b$		$t = -91^{\circ}c$ $P = 0.9$ kbar $X = 97\%$	$t = 40^{\circ}$ $P = 1.8$ kbar $X = 98\%$	$t = 18.6^{\circ}$ $P = 1.85$ kbar $X = 58\%$	$t = -21.9^{\circ}d$ $P = 2.05$ kbar $X = 31.5\%$
Q ₄ ^h	$i_{(m)}h_{17}lh_7$	-14.8° 1.15 kbar 10%	-23.4° 2.40 kbar 8.5%	-20° 2.85 kbar 1%	-21° 2.97 kbar 11%	-24.8° 2.5 kbar 14%
Q ₅ ^h	h_7h_mls		-69° 3.9 kbar 97%	-40° 4.9 kbar 98%	-5.8° 4.0 kbar 46%	
Q ₆ ^h	$i_{(m)}lh_7h_m$		-9° 5.1 kbar 9.5%	-1.5° 6.1 kbar 2%	-7.5° 5.6 kbar 19.0%	
Q ₅	$ilh_m s$ or $ih_m ls$				25° 10.6 kbar 14%	-17.5° 4.05 kbar 12%
C ₁₇	$ih_{17}l^e$ $x_{h_{17}} = x_{i^o}$	-9.6° 0.1 kbar 15.6%	$-2.4^{\circ}e$ 1 bar 19.5%	$5.0^{\circ}e$ 1 bar 19.1%	$-2.85^{\circ}e$ 1 bar 22.3%	-12.0° 0.57 kbar 22.3%
C ₁₇	$h_{17}l^o/h_7$ $x_{i^o} = x_{h_{17}}$	-12.7° 0.7 kbar 15.6%	-13.0° 1.9 kbar 19.47%	-7.0° 2.35 kbar 19.10%	-15.3° 2.43 kbar 22.34%	-23.1° 2.3 kbar 22.34%

C_7	$h_{17}l^o h_7$ $x_{i^o} = x_{h_7}$	-14.5° 0.25 kbar 31%	-13.0° 1.6 kbar 40.7%	-5.0° 2.05 kbar 36.1%	-14.0° 2.05 kbar 38.95%
C_7^i	$h_7 l^o h_m$ $x_{i^o} = x_{h_7}$	-1.9° 4.4 kbar 40.7%	-1.9° 4.4 kbar 40.7%	10.0° 5.25 kbar 36.1%	-4.75° 4.2 kbar 38.95%
C_m	$h_7 l^o h_m$ $x_{i^o} = x_{h_m}$	-2.3° 4.2 kbar 50.7%	-2.3° 4.2 kbar 50.7%	10.0° 5.15 kbar	
E_1	$i_1 h_{17}$	-3.7° 1 bar 10%	-3.7° 1 bar 10%	-1.0° 1 bar 5%	-3.45° 1 bar 14.5%
Π_1	$i_1 h_{17} l$				-11.3° 1 bar 37%
E_2	$h_{17} l s$	-99° 1 bar 98%	-99° 1 bar 98%	-110° 1 bar 97.5%	-42.3° 1 bar 97.5%

^a h_j - hydrate with hydrate number j ; i - ice, Roman numerals designate ice modification; s - solid hydrateformer; l - liquid phase; l^o - liquid phase with the composition of the hydrate that is in equilibrium with it.

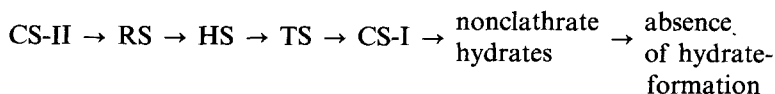
^bPhases are arranged in the order of increase of the hydrate former content.

^cDue to the presence in this system at normal pressure of hydrate h_R phases h_R, h_7 coexist at the point Q_3^h , in addition, point Q_4^h appears ($t = 17.5^\circ$, $P = 1.3$ kbar, $x = 75\%$ with phases h_{17}, h_R, h_7, l).

^dThe phases in this point are arranged as follows: $h_{17} l h_7 s$.

^eHydrate h_{17} melts congruently at normal pressure; l^o - the composition of the liquid equal to that of the equilibrium hydrate.

following scheme:



rather than from the most friable CS-II hydrates (h_{17}) immediately to the densest CS-I hydrates (h_7 or h_m). However, the frameworks of the above structures possess greater energy capacity, and occur rarely, even at 1 bar and with molecules of certain (stretched) shapes. Therefore, they are much less likely to appear and to be found under pressure. The transition from CS-II to CS-I hydrates generally occurs at increased pressures.

In this connection it is interesting to follow the development of the idea of CS-I and CS-II clathrate hydrates and their relationship. In 1951 Claussen [40], not content with the gas hydrate structures proposed by Stackelberg [12], with the help of modelling found a cubic structure with a parameter equal to 17 Å, which we now call CS-II, and explained the then available data on $M \cdot 17 \text{H}_2\text{O}$ hydrates stoichiometry by filling only the big cavities. Stackelberg confirmed this structure by the X-ray structural technique and pointed to the existence of one more cubic structure with a parameter of 12 Å [41, 42]. Independently this structure was discovered by Pauling and Marsh [43]. Since that time an idea persisted that gas clathrate hydrates have one of these structures: small molecules with dimensions up to 5.6 Å produce CS-I hydrates and bigger molecules (5.8–6.6 Å) produce CS-II¹¹. With molecules of an intermediate size changing the conditions makes it possible to obtain hydrates of both structures [2, 4, 47]. As follows from the present work, it has been established that in all the systems with the formation of CS-II hydrates at normal pressure, CS-I hydrates form under pressure, which indicates the similarity of these structures. Finally, Davidson's school has shown that very small species, such as Ar, Kr, O₂ and N₂ [25, 27] can stabilize CS-II (but with the filling of the small cavities¹², too), rather than CS-I. Thus, after a third of a century, Claussen's view on filling both types of cavities in CS-II by one kind of molecules has been verified.

In conclusion we will note that clathrate hydrates presumably have not only a lower pressure and upper temperature limit, which is natural, but also an upper pressure limit, as is clear from the present work. Besides, many hydrates also have a lower temperature limit, which follows from the work of Davidson *et al.* [25, 48].

Acknowledgement

The authors gratefully acknowledge the work of N. V. Udachina in translating this report into English.

Notes

¹Independently, but a little later we studied the melting of a number of clathrate hydrates (including the THF hydrate) under pressure [13]. The results proved to be in good agreement with the data of [11]. Dr. Davidson kindly called our attention to this fact in his letter of June 6, 1974.

²M. Stackelberg considered the hydrophobic nature of the guest molecule [12] to be one of the essential conditions for clathrate hydrate formation. However as shown later by Stackelberg himself [12a] weak

hydrophilic bonds, facilitating the hydrate former solubility in a liquid phase (e.g., in the systems with CO_2 , SO_2 , cyclic ethers, ketones, etc) break: van der Waals interactions provided by a great number of contacts, when the packing of the guest and the host is favourable, proves to be more advantageous.

³We proceed from the experimental fact that at 1 bar all the large cavities are occupied. (For this reason it is of no importance whether they are fully occupied, as we believe is the case [23], or only almost fully occupied, as is stated in the work of D. Davidson *et al.* [24].

⁴We mean CS-II hydrates with big guest molecules not capable of being accommodated in D-cavities in contrast to very small species (Ar, Kr, O_2 , N_2) [25–27], which can also stabilize CS-II hydrates, filling both big and small cavities. The packing coefficients of this kind of hydrate and CS-I hydrates are approximately equal if their filling degrees are the same.

⁵The packing coefficient depends not only on the number, but also on the efficiency of filling of each cavity volume by a guest molecule. However, variations due to the latter condition have a narrower range, since clathrate formation itself presupposes a good guest molecule and host cavity complementary ability.

⁶In many systems (e.g., in those with tetrahydrofuran, 1,3-dioxane, 1,3-dioxolane, etc) the point C_{17} is found at pressures below normal and appears when the hydrate and the liquid phase composition in the equilibrium $h_{17} \rightleftharpoons 1 + g$ become equal.

⁷To use conventional designation (point Q_1 – equilibrium ihg and Q_2 – equilibrium $1, hl_2g$) we begin our description from the point Q_3^h , the index h is used for the points where the equilibrium with two hydrates is realized.

⁸The packing coefficients of clathrate hydrates (0.47–0.59) are greater than those of ice Ih (0.43), but significantly smaller than those of substances with denser packing (0.70–0.74), which are approached by high pressure ices and, as one may suppose, 1,4-dioxan.

⁹The 1,3-dioxolane system is peculiar (though this is not of fundamental importance here) in that at 1 bar, in addition to h_{17} , one more hydrate h_R , destabilized by pressure, forms in it, which results in two nonvariant points instead of one (see Table II).

¹⁰Since the 1,4-dioxane melting point is relatively high ($t = +11.2^\circ\text{C}$) and it increases very rapidly under pressure ($\gamma = 22.6^\circ/\text{kbar}$), its crystallization field grows rapidly and overlaps the hydrate h_7 crystallization field to a considerable extent. The 1,3-dioxane–water system makes up for this ‘disadvantage’.

¹¹Rare exceptions are observed for molecules of oblong shape (bromine [44] dimethyl ether [45]) for which tetragonal syngony hydrates have been found and formation of hexagonal structure hydrates is also possible [46] with the stoichiometry $\text{Br}_2 \cdot 10 \text{H}_2\text{O}$. One more hexagonal structure has recently been discovered [56] in which for every large 20-hedral cavity (E) occupied by methylcyclohexane there are five small ones, occupied by hydrogen sulphide. This kind of structure can exist only as a double hydrate [53]. This formula of the unit cell is $\text{E} \cdot 3\text{D} \cdot 2\text{D}' \cdot 34 \text{H}_2\text{O}$, where D is a pentagonal dodecahedron, D' is a dodecahedron; $4^3 5^6 3$.

¹²The phenomenon of CS-II hydrates being stabilized by small molecules of a help gas is well known. For instance, acetone hydrate $\text{Ac} \cdot 17 \text{H}_2\text{O}$ melts at -20°C , but at 1 bar Xe, it melts at $+2^\circ\text{C}$. In several cases (e.g. with COS hydrates) an auxiliary gas causes CS-I hydrate to change into CS-II [24]. In the case of hydrates of Ar, Kr and other substances something like ‘self-stabilization’ of CS-II hydrates occurs [25].

References

1. D. F. Sargent and L. D. Calvert: *J. Phys. Chem.* **70**, 2689 (1966).
2. R. E. Hawkins and D. W. Davidson: *J. Phys. Chem.* **70**, 1889 (1966).
3. L. Carbonnel and J. -C. Rosso: *Rev. Chem. Miner.* **9**, 771 (1972).
4. S. R. Gough, S. K. Garg, and D. W. Davidson: *J. Chem. Phys.* **3**, 239 (1974).
5. O. Maass and E. H. Broomer: *J. Am. Chem. Soc.* **44**, 1709 (1922).
6. H. A. Palmer: *Proc. Okla. Acad. Sci.* **30**, 1400 (1949), cit. from. [7].
7. J. Erva: *Suomen Kemist.* **10**, 29B, 183 (1956).
8. B. D. Thorpe and K. L. Pinder: *Suomen Kemist.* **38**, 243 (1965).
9. R. K. McMullan and G. A. Jeffrey: *J. Chem. Phys.* **42**, 2725 (1965).
10. T. C. W. Mak and R. K. McMullan: *J. Chem. Phys.* **42**, 2732 (1965).
11. S. R. Gough and D. W. Davidson: *Can. J. Chem.* **49**, 2691 (1971).
12. M. Stackelberg: *Naturwiss.* **36**, 327 (1949).

- 12.a. M. Stackleberg and B. Meuthen: *Z. Electrochem.* **62**, 130 (1958).
13. Yu. A. Dyadin, P. N. Kuznetsov, I. I. Yakovlev, and A. V. Pyrinova: *Dokl. Akad. Nauk SSSR* **208**, 103 (1973); *C.A.* **78**, 102558r (1973); *Izv. Sib. Otd. Akad. Nauk. SSSR. Ser. khim. nauk*, **4**, 3 (1972) *C.A.* **77**, 1566070d (1972).
14. Yu. A. Dyadin, P. N. Kuznetsov, and I. I. Yakovlev: *Izv. Sib. Otd. Akad. Nauk SSSR. Ser. khim. nauk.* **2**, 30 (1976). *C.A.* **84**, 156307a (1976).
15. Yu. M. Zelenin, Yu. A. Dyadin, and F. V. Zhurko: *VINITI, N 5239 Dep.* (1984).
16. Yu. A. Dyadin, I. V. Bondaryuk, G. L. Rijikova, Ye. Ya. Aladko, and Yu. M. Zelenin: *Izv. Sib. Otd. Akad. Nauk SSSR. Ser. khim. nauk.* **8**, 67 (1984). *C.A.* **101**, 64836p (1984).
17. Yu. A. Dyadin, P. N. Kuznetsov, and I. I. Yakovlev. *Izv. Sib. Otd. Akad. Nauk. SSSR, Ser. khim. nauk.* **7**, (1975). *C.A.* **83**, 183514b (1975).
18. B. Bartok: *Acta. Univ. Szeged., Acta Phys. Chem.* **8**, 133 (1962).
19. D. S. Tsiklis: *Tekhnika fiziko-khimicheskikh issledovaniy pri visokikh i sverkhvisokikh davelniyakh.* M. Khimia (1976).
20. V. S. Bogdanov and A. P. Miroshnikov: *Trudi metrologicheskikh institutov SSSR.* M; **104**, 33 (1969).
21. J. -C. Rosso and L. Carbonnel: *C.R. Acad. Sci. Paris* **274**, 1108 (1972).
22. A. I. Kitaygorodskii: *Smeshanyi Kristally.* Nauka, 276 (1983).
23. Yu. A. Dyadin and K. A. Udachin: *J. Incl. Phenom.* **2**, 61 (1984).
24. D. W. Davidson: 'Clathrate Hydrates'. Ch. 3 in *Water. A Comprehensive Treatise*, vol. 2, N.-Y, London, p. 115 (1973).
25. D. W. Davidson, S. K. Garg, and Y. P. Handa: *J. Incl. Phenom.* **2**, 231 (1984).
26. D. W. Davidson. Y. P. Handa, C. J. Ratcliffe, and J. A. Ripmeester: *Mol. Cryst. Liq. Cryst.* **141**, 141 (1986).
27. D. W. Davidson and Y. P. Handa: *Nature* **311**, 5982, 142 (1984).
28. R. G. Ross and P. Andersson: *Can. J. Chem.* **60**, 881 (1982).
29. R. G. Ross and P. Andersson: *Nature* **290**, 5804, 322 (1981).
30. I. I. Novikov: *Dokl. Akad. Nauk SSSR.* **100**, 1119 (1955).
31. D. N. Glew and N. S. Rath: *J. Chem. Phys.* **44**, 1710 (1966).
32. R. K. McMullan and G. A. Jeffrey: *J. Chem. Phys.* **42**, 2725 (1965).
33. J. E. Bertie and S. M. Jacobs: *J. Chem. Phys.* **69**, 4105 (1978).
34. K. W. Morcom and R. W. Smith: *J. Chem. Thermodyn.* **3**, 507 (1971).
35. D. W. Davidson, S. R. Gough, F. Lee, and J. A. Ripmeester: *Rev. Chim. Miner.* **447**, 14 (1977).
36. H. Nakayama and M. Tahara: *Bull. Chem. Soc. Jpn.* **46**, 2965 (1973).
37. S. R. Gough, J. A. Ripmeester, and D. W. Davidson: *Can. J. Chem.* **53**, 2215 (1975).
38. L. V. Vilkov, V. S. Mastryukov, and N. I. Sadova: *Opreделение geometricheskogo stroeniya svobodnikh molekul.* M., Khimia (1978).
39. Yu. V. Zefirov and P. M. Zorkii: *Zh. Struct. Khim.* **15**, 118 (1974).
40. W. F. Claussen: *J. Chem. Phys.* **19**, 259 (1951).
41. M. Stackelberg: *J. Chem. Phys.* **19**, 1319 (1951).
42. M. Stackelberg: *Angew. Chem.* **64**, 423 (1452).
43. L. Pauling and R. E. Marsh: *Proc. Acad. Sci.* **38**, 112 (1952).
44. K. W. Allen and G. A. Jeffrey: *J. Chem. Phys.* **38**, 2304 (1963).
45. S. L. Miller, S. R. Gough, and D. W. Davidson: *J. Phys. Chem.* **81**, 2154 (1977).
46. Yu. A. Dyadin and L. S. Aladko: *Zh. Strukt. Khim.* **18**, 51 (1977). *C.A.* **87**, 12297m (1977).
47. D. R. Hafemann and S. L. Miller: *J. Phys. Chem.* **73**, 1392 (1969).
48. S. L. Miller and W. D. Smythe: *Science* **170**, 533 (1970).
49. F. V. Zhurko, G. G. Zhurko, and Yu. A. Dyadin: *Izv. Sib. Otd. Akad. Nauk SSSR. Ser. khim. nauk.* **5**, 72 (1989).
50. Y. P. Handa, R. E. Hawkins, and J. J. Murray: *J. Chem. Thermodyn.* **16**, 623 (1984).
51. Y. P. Handa: *J. Chem. Thermodyn.* **17**, 201 (1985).
52. Y. P. Handa: *Can. J. Chem.* **63**, 68 (1985).
53. Y. P. Handa C. I. Ratcliffe, J. A. Ripmeester, and J. S. Tse: *Abstracts of Gas Hydrate Symposium*, Toronto, June 1988.
54. D. W. Davidson, S. R. Gough, F. Lee, and J. A. Ripmeester: *Rev. Chem. Min.* **14**, 447 (1977).
55. J. E. Bertie and S. M. Jacobs: *Can. J. Chem.* **55**, 1777 (1977).
56. J. A. Ripmeester, J. S. Tse, J. R. Christopher, and B. M. Powell: *Nature* **325**, 135 (1986).